RESEARCH ARTICLE

Polyploid Titan Cells Produce Haploid and Aneuploid Progeny To Promote Stress Adaptation

Aleeza C. Gerstein,[a,b,c] Man Shun Fu,[a] Liliane Mukaremera,[a] Zhongming Li,[a] Kate L. Ormerod,[d] James A. Fraser,[d] Judith Berman,[a,b,c] Kirsten Nielsen[a]

Department of Microbiology and Immunology, Medical School, University of Minnesota, Minneapolis, Minnesota, USA[a]; Department of Molecular Microbiology and Biotechnology, George S. Wise Faculty of Life Sciences, Tel Aviv University, Israel[b]; Department of Genetics, Cell Biology & Development, College of Biological Sciences, University of Minnesota, Minneapolis, Minnesota, USA[c]; Australian Infectious Diseases Research Centre, School of Chemistry and Molecular Biosciences, University of Queensland, Brisbane, Queensland, Australia[d]

A.C.G. and M.S.F. contributed equally to this article.

ABSTRACT ***Cryptococcus neoformans*** **is a major life-threatening fungal pathogen. In response to the stress of the host environment, *C. neoformans* produces large polyploid titan cells. Titan cell production enhances the virulence of *C. neoformans*, yet whether the polyploid aspect of titan cells is specifically influential remains unknown. We show that titan cells were more likely to survive and produce offspring under multiple stress conditions than typical cells and that even their normally sized daughters maintained an advantage over typical cells in continued exposure to stress. Although polyploid titan cells generated haploid daughter cell progeny upon *in vitro* replication under nutrient-replete conditions, titan cells treated with the antifungal drug fluconazole produced fluconazole-resistant diploid and aneuploid daughter cells. Interestingly, a single titan mother cell was capable of generating multiple types of aneuploid daughter cells. The increased survival and genomic diversity of titan cell progeny promote rapid adaptation to new or high-stress conditions.**

IMPORTANCE **The ability to adapt to stress is a key element for survival of pathogenic microbes in the host and thus plays an important role in pathogenesis. Here we investigated the predominantly haploid human fungal pathogen *Cryptococcus neoformans*, which is capable of ploidy and cell size increases during infection through production of titan cells. The enlarged polyploid titan cells are then able to rapidly undergo ploidy reduction to generate progeny with reduced ploidy and/or aneuploidy. Under stressful conditions, titan cell progeny have a growth and survival advantage over typical cell progeny. Understanding how titan cells enhance the rate of cryptococcal adaptation under stress conditions may assist in the development of novel drugs aimed at blocking ploidy transitions.**

Received 6 August 2015 **Accepted** 23 September 2015 **Published** 13 October 2015

Citation Gerstein AC, Fu MS, Mukaremera L, Li Z, Ormerod KL, Fraser JA, Berman J, Nielsen K. 2015. Polyploid titan cells produce haploid and aneuploid progeny to promote stress adaptation. mBio 6(5):e01340-15. doi:10.1128/mBio.01340-15.

Editor Gary B. Huffnagle, University of Michigan Medical School

Address correspondence to Kirsten Nielsen, knielsen@umn.edu.

The ability to acclimate and adapt to a changing environment is key for survival in all organisms. The opportunistic fungal pathogen *Cryptococcus neoformans* is ubiquitous in the environment and enters the host following inhalation of spores or desiccated yeast cells into the lungs (1). The change experienced by the cryptococcal cells during the transition from the external environment to the host is dramatic, involving multiple stressors such as higher temperature, lower oxygen levels, lower iron levels, and high levels of free radicals generated by the host immune response. This transition stimulates the rapid upregulation of genes involved in stress responses and virulence (2), and only a small proportion of colonizing cells survive (3).

Upon exposure to the host lung, *C. neoformans* produces large polyploid titan cells. Typical cryptococcal cells are 5 to 7 μm in diameter and have a haploid (1C) genome; in contrast, titan cells can be 5 to 10 times larger than normal cells and are predominantly tetraploid (4C) or octoploid (8C), with higher ploidies also frequently observed (4, 5). Although large cryptococcal cells have long been noted during human infection (6, 7), they have only recently begun to be characterized in depth through *in vitro* study, mouse experiments (4, 5), and clinical histological studies (8). As the morphology of titan cells is quite different from that of typical cells, clinical misdiagnosis or underdiagnosis may be common (8) and the true extent of titan cell prevalence and of the impact on human disease remains to be determined.

Polyploid titan cells can be detected in mouse lung tissue within 1 day postinfection; the frequency of titan cells typically plateaus at ~20% of the cryptococcal cell population in the lungs within 7 days (4). The morphology of titan cells differs significantly from that of typical cells. The titan cell wall is much thicker than that of typical cells, and the titan cell capsule is both denser and more cross-linked (9). These differences promote titan cell survival in the mouse host through reduced phagocytosis and production of a detrimental Th2-mediated immune response (10, 11). Importantly, titan cells are critical for survival within the mouse host and for causing subsequent disease (3–5, 11, 12).

Whether the survival advantage of titan cells over typical cells *in vivo* is due to their morphological differences, their increased size, or their increased ploidy (or to a combination of these factors) remains unknown.

Ploidy variation within species and among cell types within an individual is surprisingly common among fungal microbes. Polyploid individuals have been sampled in natural isolates of *Saccharomyces cerevisiae* (13), among clinical isolates of *Candida albicans* (14), and even within nuclei that share a cytoplasm in *Ashbya gossypii* (15). Developmentally programmed endoploidy (duplication of the genome without division during mitosis) also regularly appears in the *Plantae*, *Animalia*, and fungal kingdoms among a subset of cells as a response to physiological stress, in resource-limited settings, or as a means to ward off DNA damage (8, 11–13). Furthermore, the signature of paleopolyploidy is prevalent among many sequenced eukaryotic genomes (16) and all sexual species, by definition, undergo ploidy shifts during their life cycles (17). Changes in ploidy (independently of other genetic changes) directly affect cell size (18) and gene expression (19–24) and may act as a mechanism to divert energy away from cell division into the production of proteins (19, 25).

Polyploidy can also lead to the rapid accumulation of genetic diversity within populations, as polyploid genomes are often highly unstable. Offspring of polyploid cells frequently carry chromosomal rearrangements and translocations and exhibit amplification of chromosomal segments or whole-chromosome aneuploidy (26–29). These major structural changes often incur a fitness cost under normal growth conditions (30) and yet can be beneficial under certain conditions. Cancer cells exhibiting a high frequency of aneuploidy are associated with rapid cell growth (31–35), and some aneuploidies confer resistance to chemotherapeutic drugs (36, 37). Several recent studies in yeasts show that aneuploidy may also promote adaptation to a diversity of stress conditions (21, 38–43). Unlike polyploidization, which is predicted to maintain gene expression dosage ratios across the genome, specific chromosomal aneuploidies can be advantageous through selection for increased gene expression of a subset of genes. In *C. albicans*, for example, 50% of isolates resistant to the antifungal drug fluconazole carried at least one aneuploid chromosome and many had a specific aneuploidy, isochromosome (5L), that contains two genes (*ERG11* and *TAC1*) that confer fluconazole resistance upon overexpression (36). Likewise, fluconazole-resistant strains in *C. neoformans* frequently contain extra copies of chromosomes 1, 4, 10, and 11 (42, 44), and high levels of Chr12 aneuploidy have also been reported in clinical isolates (45). Yet the factors that influence the rate of aneuploidy formation remain largely unknown.

Here we asked whether titan cells enhance the ability of cryptococcal populations to survive and adapt to stress conditions. Using population-level experiments, we found that populations of titan cells have a survival advantage over typical cells in multiple environments. Furthermore, the normally sized daughter progeny of titan cells maintained a growth advantage relative to the daughters of typical cells when grown in fluconazole. Interestingly, titan cell offspring produced in the presence of stress are both resistant to stress and genotypically variable, often carrying multiple chromosomal aneuploidies.

RESULTS

Titan cell cultures survive stress conditions better than typical cells. To study the survival of titan cells relative to the survival of normally sized ("typical") cells in the presence of physiologically relevant stressors, we isolated and cultured purified titan and typical cell populations with different degrees of oxidative stress (H_2O_2) and nitrosative stress ($NaNO_2$) and with treatment with the antifungal drug fluconazole, which targets ergosterol biosynthesis (46). Titan cell survival exceeded that of typical cells at several levels of each stressor, with the precise relationship being dependent upon the environment tested (Fig. 1; see also Table S1 in the supplemental material). With fluconazole stress, titan cells had a survival advantage at high levels of fluconazole and yet responded similarly to lower levels of drug. With oxidative stress, in

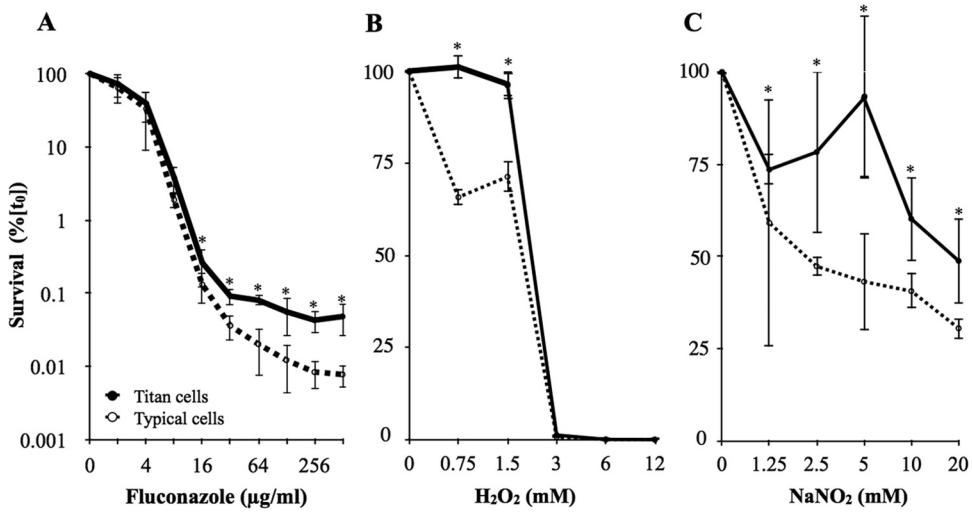

FIG 1 Titan cell cultures show increased resistance to multiple stresses. Typical and titan cells were isolated *in vivo* and grown in (A) YPD broth supplemented with antifungal drug (fluconazole) or in RPMI broth supplemented with (B) H_2O_2 (oxidative stress) or (C) $NaNO_2$ (nitrosative stress). Aliquots from each treatment were plated on YPD, and CFUs were counted. Data are normalized to cells grown in YPD or RPMI broth alone and plotted as the mean from biological triplicates with error bars indicating standard deviation. Asterisks (*) indicate the stress levels that were included in a two-way ANOVA model that showed a statistically significant difference in survival and growth between titan and typical cell populations. [$\%t_0$], percent of time 0.

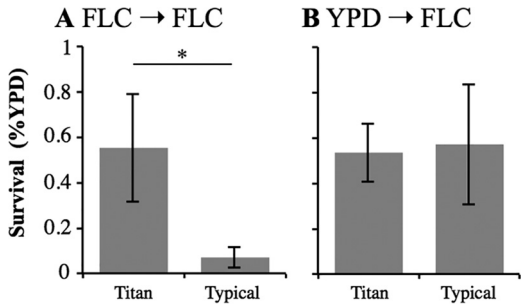

FIG 2 Titan cell populations as well as the populations of their normally sized titan daughter cells have a growth and survival advantage over typical cell populations in fluconazole. Populations of titan and typical cells were grown in (A) YPD plus fluconazole or (B) YPD. The resultant titan cell populations were filtered to remove any remaining titan-sized cells. The normally sized daughters of titan cells and the typical cell populations were then reinoculated into YPD plus fluconazole. *, $P < 0.05$.

contrast, titan cells had a significant survival advantage at lower levels of stressor but not at higher levels. With nitrosative stress, the titan cell advantage was seen across all levels tested. Interestingly, the number of titan cells present within the cultures under these stress conditions did not increase following incubation; rather, the populations were dominated by normally sized (5-μm to 7-μm diameter) cells after incubation under stress conditions. These data are consistent with titan cells producing normally sized daughter cells upon replication (4).

To characterize the molecular mechanisms underlying the stress resistance of the titan daughter cell populations, we explored resistance to the antifungal drug fluconazole in more detail. To determine whether the presence of the titan cells was required, we examined the fluconazole resistance of the normally sized offspring of titan cells grown in the presence of fluconazole (Fig. 2). We grew both typical and titan cells in the presence of 128 μg/ml fluconazole and isolated their normally sized daughter cells via filtration. If the initial increase in fluconazole resistance was due to features of the titan cells themselves, then their purified normally sized daughter cells should have behaved the same as the offspring of typical cells. Importantly, the growth advantage afforded to titan cells in fluconazole (Fig. 1A) was maintained even in comparison of the growth of their normally sized daughters to that of typical daughter cells after a second round of growth in fluconazole (Fig. 2A; two-way analysis of variance [ANOVA]) (type, $F_{1,23} = 5.08$, $P = 0.034$; experiment day, $F_{1,23} = 0.47$, $P = 0.50$). This indicates that the survival advantage of titan cells is passed along to their normally sized daughters when growth in fluconazole is maintained. In contrast, when typical and titan cell populations were first grown in yeast extract-peptone-dextrose (YPD), there was no difference between the progeny of the typical cells and the titan cell daughter progeny upon exposure to fluconazole (Fig. 2B; two-way ANOVA) (type, $F_{1,23} = 0.69$, $P = 0.42$; experiment day, $F_{1,23} = 1.84$, $P = 0.19$). These data suggest that prior and continued exposure of titan cells to a stress somehow provides the normally sized titan progeny cells with an enhanced ability to survive the same stress.

The increased fluconazole resistance of titan daughter cells could be due to selection for a subset of the original titan cells or could be a general effect seen for all titan cells. To distinguish between these possibilities, we examined the ability of individual titan cells to produce fluconazole-resistant progeny. Single titan and typical cells were micromanipulated onto YPD plates in both the presence and absence of 8 μg/ml fluconazole (note that the drug concentration in plates is not directly comparable to the drug concentration in liquid). In this assay, only progeny that are able to both survive and divide generate colonies. In the absence of fluconazole, there was no difference between titan and typical cells in colony growth results (77% survival in both cases; Table 1). However, titan cells were much more likely than typical cells to produce colonies in the presence of fluconazole (17.5% of titan cells compared to only 3% of typical cells; $P < 0.0001$ by Fisher's exact test; Table 1). Taken together, these data show that titan cells were more likely to survive and generate progeny in the presence of stress and also that their normally sized titan daughter cells inherit this stress resistance advantage.

Genomic basis of stress resistance. The observed stress resistance of the titan daughter cell populations suggested a heritable mechanism of resistance. We first examined ploidy of the titan daughter cells from titan cells cultured under nutrient-replete and stress conditions. Purified titan cells were isolated by filtration from bronchoalveolar lavage (BAL) fluid and cultured using nutrient-replete medium for 24 h (~11 generations). Flow cytometry analysis of the cell populations revealed that while the vast majority (>80%) of the starting cells were polyploid titan cells (with a diameter of ≥15 μm and >1C DNA content) (Fig. 3A and B), the titan progeny were almost exclusively <15 μm in diameter, with flow profiles consistent with haploidy (Fig. 3B). Thus, titan mother cells rapidly gave rise to populations of haploid progeny in the absence of stress.

To follow the growth trajectories of specific titan mothers and their progeny, five individual titan cells were macromanipulated

TABLE 1 Increased survival of titan progeny under conditions of fluconazole stress

Cell type	FLC[a]	No. of cells analyzed[b]			No. of resulting colonies[c]			Growth (% ± SD)[d]	Growth normalized to no-treatment conditions (% ± SD)[e]
		1	2	3	1	2	3		
Titan	−	40	40	50	29	29	42	76.3 ± 6.6	
	+	145	138	100	26	22	19	17.6 ± 1.6	23.1 ± 0.1*
Typical	−	40	40	50	27	30	42	75.5 ± 8.3	
	+	145	150	150	3	4	6	2.9 ± 1.0	3.9 ± 0.4*

[a] FLC, fluconazole. The concentration of fluconazole was 8 μg/ml.
[b] Data represent the total numbers of single cells microdissected on YPD with or without fluconazole in three independent experiments.
[c] Data represent the numbers of colonies of titan and normally sized cells from microdissected cells in three independent experiments.
[d] Data represent the proportions of microdissected cells that generated colonies. Data are expressed as averages of the percentages from the three experiments ± standard deviation.
[e] Data represent the proportions of the microdissected cells that generated colonies on fluconazole normalized to the proportion generated on YPD. *, $P < 0.05$.

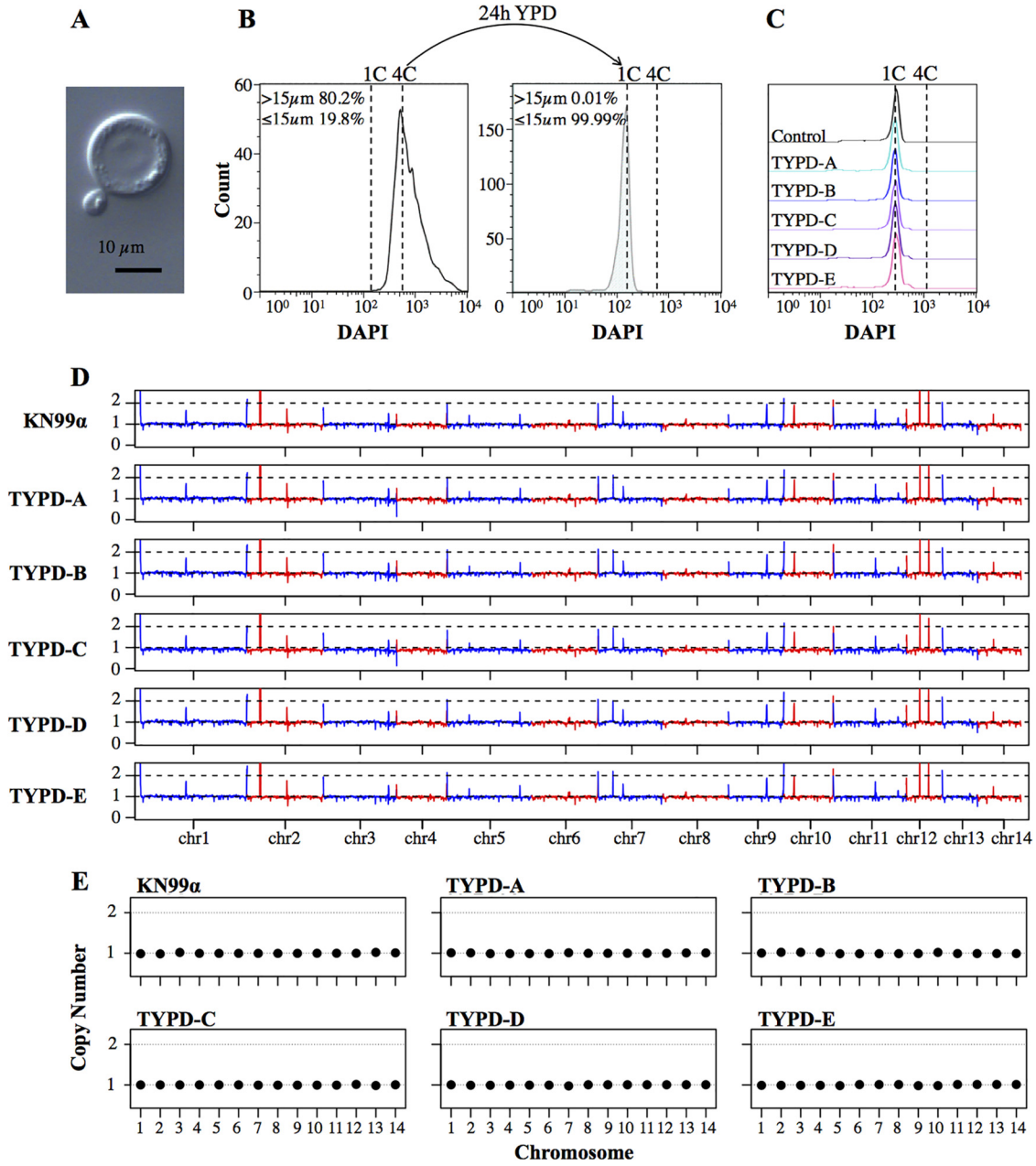

FIG 3 Titan cells generate haploid progeny under nutrient-replete conditions. (A) Titan cell replication in YPD medium, showing a titan cell and its daughter cell. Bar = 10 μm. (B) DNA content of purified titan cells at the time of isolation (4C) and following culture in YPD medium (1C) analyzed by flow cytometry using DAPI staining. The numbers in the upper left corner of each panel represent the percentages of cells >15 μm or ≤15 μm in diameter in the culture. (C) Single titan cells were microdissected on YPD agar, and the DNA content of the resulting colonies was analyzed by flow cytometry. (D) Whole-genome sequence analysis of colonies generated from single titan cells grown on YPD (TYPD). Chromosomal (chr) copy numbers were defined based on the depth of sequence coverage across each chromosome in 1,000-bp bins compared to the data from haploid KN99α cells grown *in vitro*. Different chromosomes are indicated in alternating red and blue. (E) Average ploidy for each chromosome determined from the mean depth of sequence coverage across all reads mapped to each chromosome.

on YPD agar plates and incubated at 30°C for 48 h to produce colonies. Consistent with the population experiment, the characteristics of the cells from the resultant colonies were overwhelmingly consistent with haploidy (Fig. 3C). Quantitative PCR (qPCR) analysis of one gene on each chromosome and multiplex PCR were first used in preliminary studies to estimate the chromosome copy number for each of the strains generated from single titan cells, and no evidence of aneuploidy was found. Higher-resolution whole-genome resequencing analysis, normalized to haploid progenitor KN99α data, confirmed that all of these titan cell progeny populations had rapidly undergone genome reduction to haploidy (Fig. 3D; qPCR results not shown). Thus, polyploid titan cells generate euploid haploid progeny under nutrient-replete, nonstress conditions.

Several studies have shown that specific aneuploid chromosomes confer fluconazole drug resistance in pathogenic fungi (42,

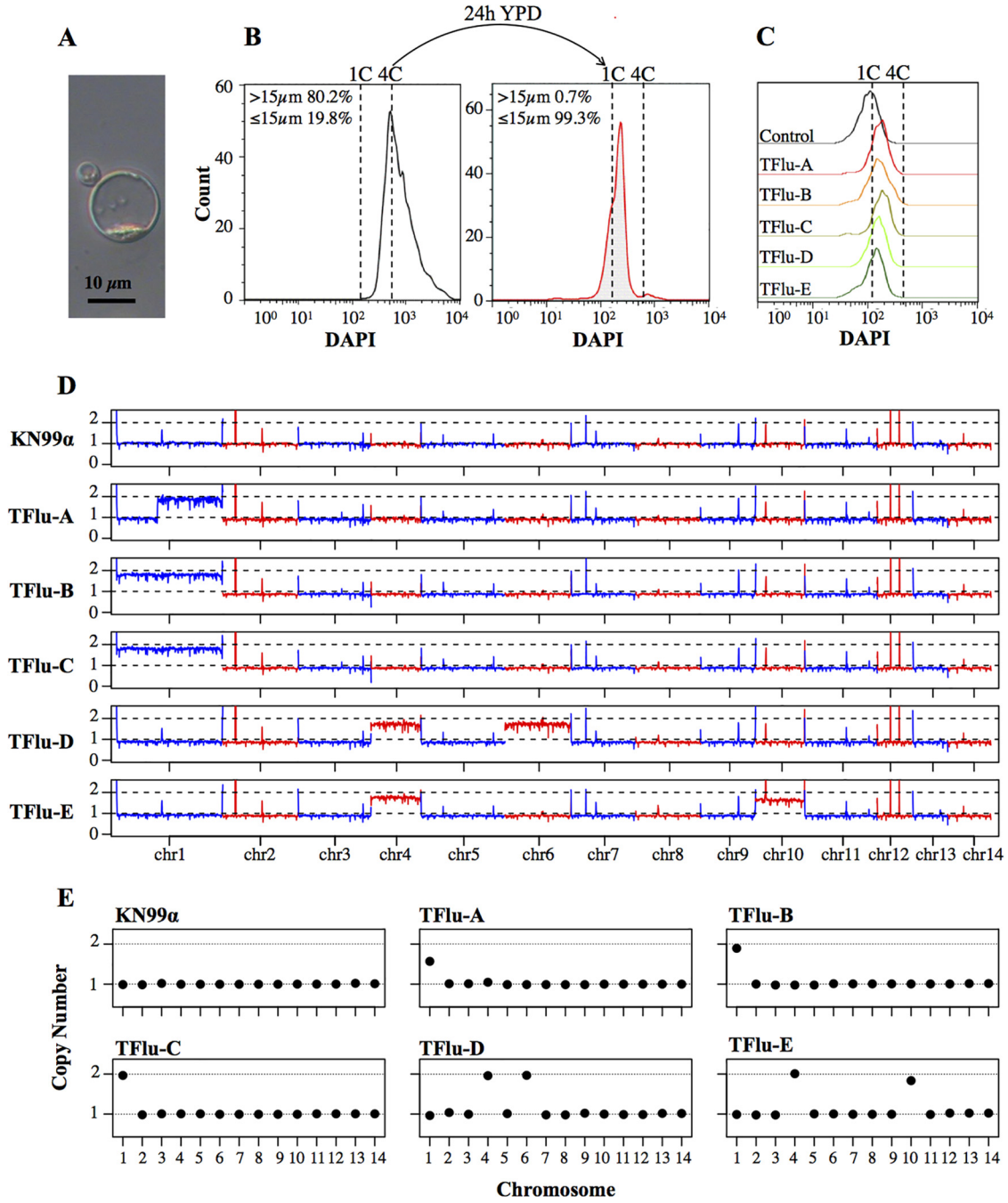

FIG 4 Titan cells generate aneuploid progeny in response to fluconazole stress. (A) Representative titan cell budding in YPD medium containing fluconazole. (B) DNA content and percentage of purified titan cells (>15 μm in diameter) and typical cells (<15 μm) at the time of *in vivo* isolation and following *in vitro* culture in YPD medium plus fluconazole. (C) DNA content of colonies that originated from single titan cells microdissected on YPD agar containing fluconazole. (D) Whole-genome sequence analysis of genomic DNA isolated from the titan cell colonies. Chromosomal copy numbers were determined based on depth of sequence coverage across each chromosome in 1,000-bp bins compared to haploid KN99α cells grown *in vitro*. Different chromosomes are indicated in alternating red and blue. (E) The average copy number for each chromosome was determined from the mean depth of sequence coverage across all reads mapped to each chromosome.

47). Thus, we hypothesized that titan cell progeny growing in fluconazole may be aneuploid. To test this, five individual titan cells were macromanipulated onto agar plates containing 8 μg/ml fluconazole and incubated at 30°C for 48 to 96 h to generate colonies. Preliminary qPCR suggested that, in contrast to colonies grown on YPD plates, these colonies contained aneuploidy (see Tables S2 and S3 and Fig. S1 in the supplemental material). The whole-genome resequencing analysis data were consistent with the qPCR experiments and confirmed that each titan cell progeny population contained at least one aneuploid chromosome or chromosome segment (TFlu-A) (Fig. 4). Southern analysis of intact chromosomes by karyotype contour-clamped homogeneous electric

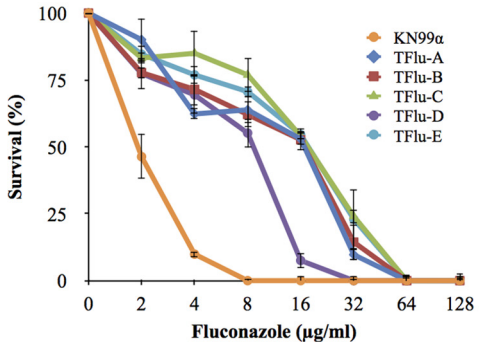

Strain	Aneuploidy	MIC_{50}	MIC_{90}
KN99α	---	2	4
TFlu-A	+Chr1R	32	32
TFlu-B	+Chr1	32	64
TFlu-C	+Chr1	32	64
TFlu-D	+Chr4, 6	16	16
TFlu-E	+Chr4, 10	32	64

FIG 5 Titan cell progeny generated in response to fluconazole have increased resistance. The data represent the growth of TFlu-A to TFlu-E and of KN99α (control) after exposure to increasing concentrations of fluconazole. Data presented are the means of triplicate biological experiments, normalized to the same strain grown in YPD, and error bars indicate standard deviations. MIC_{50} and MIC_{90} data indicate fluconazole concentrations that resulted in 50% and 90% growth inhibition, respectively. Chr, chromosome.

field (CHEF) electrophoresis of TFlu-A detected an extra 1.3-Mb band with a chr1R-specific probe (data not shown), consistent with the expected size of the extra Chr1 right-arm segment and indicative of an additional small chromosome (isochromosome) in the cells. Whole Chr1 disomy was observed in two other titan progeny populations (TFlu-B and TFlu-C), and the remaining two populations contained multiple duplications of other chromosomes: TFlu-D was disomic for Chr4 and Chr6, and TFlu-E was disomic for Chr4 and Chr10.

We next asked whether the fluconazole-resistant populations acquired other genetic changes such as chromosome rearrangements or single nucleotide variants (SNVs). CHEF gel karyotype analysis did not detect gross chromosomal rearrangements in any of the populations (data not shown). The whole-genome sequence data were then analyzed for SNVs and small indels. Six SNVs were identified across TFlu-A (2 SNVs), TFlu-B (2 SNVs), TFlu-C (1 SNV), and TFlu-E (1 SNV) compared to KN99α (see Table S4 in the supplemental material). Only three of these SNVs

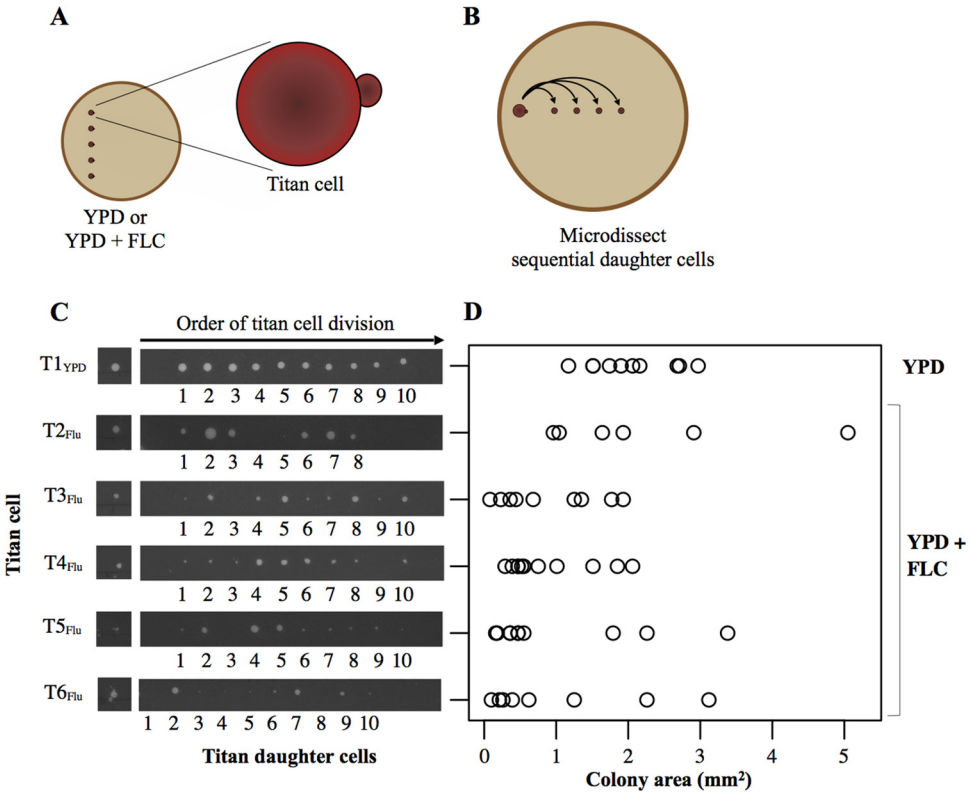

FIG 6 Single titan cells generate phenotypically variable sibling daughter cells. (A) Schematic representation of titan daughter cell isolation. Single titan cells were macrodissected onto YPD plates with or without fluconazole. (B) Individual sibling daughter cells produced from each titan cell were microdissected immediately after cell division and incubated at 30°C to generate colonies. (C) Photographs of colony size variation among individual titan daughter cells grown on YPD ($T1_{YPD}$ and YPD plus FLC) ($T2_{Flu}$ to $T6_{Flu}$); the order of titan cell division is from left to right. (D) Colony size measured for each daughter cell colony in ImageJ.

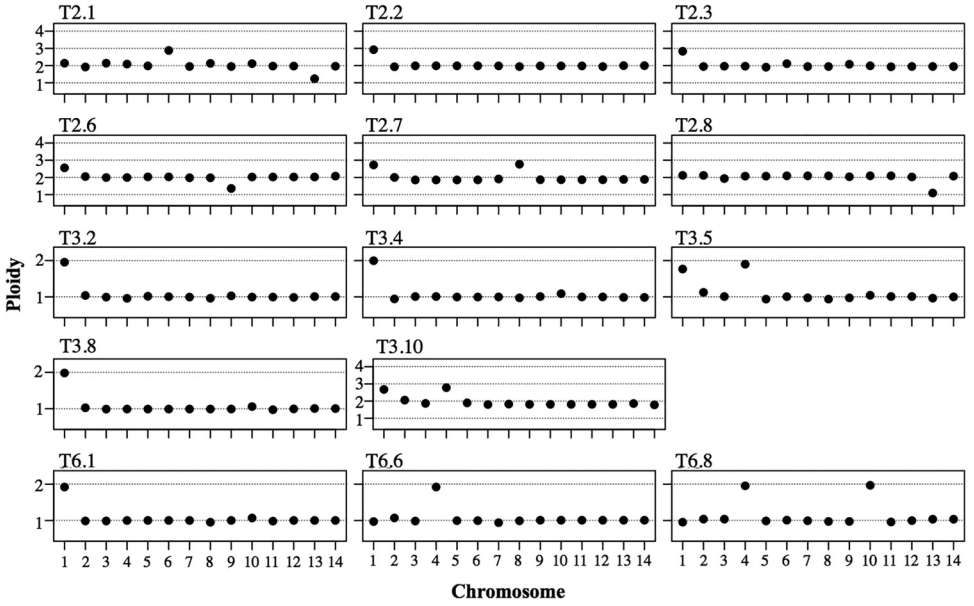

FIG 7 Titan cells generate progeny with extensive genomic diversity. Data represent results of whole-genome sequence analysis of fluconazole-resistant single titan daughter cells from titan cell strains (T2, T3, and T6); average ploidy for each chromosome determined from the mean depth of sequence coverage across all reads mapped to each chromosome is shown.

were in coding regions, and only two SNVs, both in hypothetical proteins, caused amino acid substitutions. Thus, primary-sequence single-base-pair changes were rare.

Finally, to quantitate whether the aneuploid titan cell progeny showed an increase in resistance to fluconazole relative to the progeny of parental strain KN99α, we measured MICs by microdilution assay. All five of the aneuploid progeny cultures exhibited a significantly higher drug MIC than the parent strain

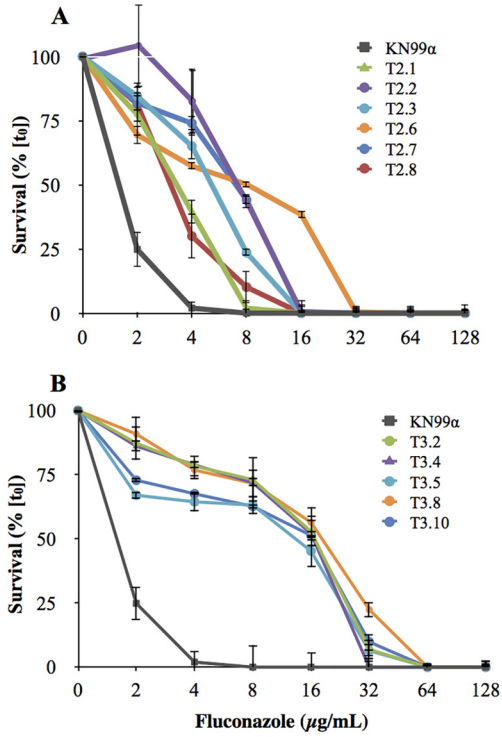

Strain	Aneuploidy	MIC_{50}	MIC_{90}
KN99α	---	2	4
T2.1	+Chr6, -Chr13	4	8
T2.2	+Chr1	8	16
T2.3	+Chr1	8	16
T2.6	+Chr1, -Chr9	16	32
T2.7	+Chr1,8	8	16
T2.8	-Chr13	4	8

Strain	Aneuploidy	MIC_{50}	MIC_{90}
KN99α	---	2	4
T3.2	+Chr1	16	32
T3.4	+Chr1	16	32
T3.5	+Chr1, 4	16	32
T3.8	+Chr1	32	64
T3.10	+Chr1, 4	32	32

FIG 8 Fluconazole resistance of titan cell progeny with different aneuploidies. Data represent growth of colonies derived from (A) sibling titan cell 2 progeny (diploid) or (B) sibling titan cell 3 progeny (haploid) after exposure to increasing concentrations of fluconazole. Data are presented as the means of the results of triplicate biological experiments, normalized to the same strain grown in YPD, and error bars indicate standard deviations. MIC_{50} and MIC_{90} data indicate fluconazole concentrations that resulted in 50% and 90% growth inhibition, respectively.

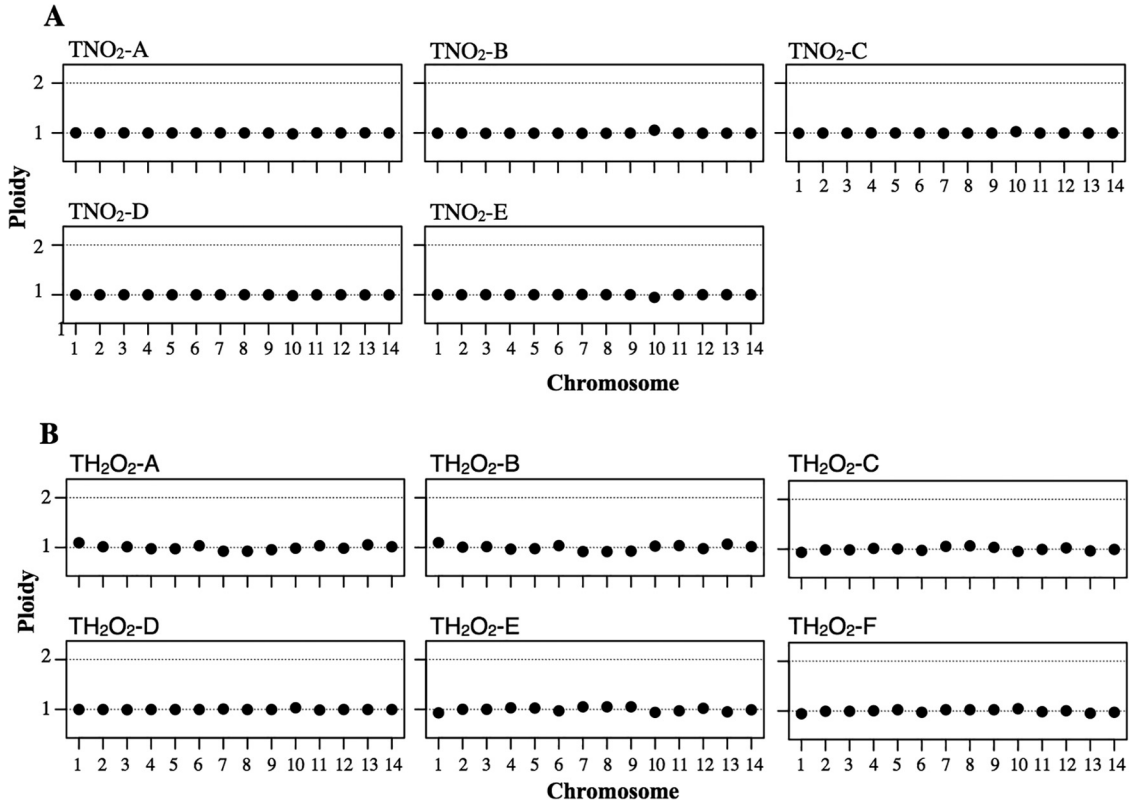

FIG 9 Titan progeny resistant to oxidative and nitrosative stress are not aneuploidy. Data represent the results of whole-genome sequence analysis of (A) oxidative-resistant and (B) nitrosative stress-resistant progeny grown from single titan cells. Average ploidy for each chromosome determined from the mean depth of sequence coverage across all reads mapped to each chromosome is shown.

(MIC_{50} values for the progeny were all either 16 μg/ml or 32 μg/ml; the MIC_{50} value for the parent strain was 2 μg/ml) (Fig. 5), indicating the rapid acquisition of increased drug resistance. Titan cells are thus capable of rapid phenotypic and genotypic change. Titan cell strains cultured under nutrient-replete conditions produced euploid haploid offspring, while titan cell strains cultured under fluconazole stress conditions produced aneuploid haploid offspring that had acquired drug resistance.

Titan cells generate sibling daughter cells with different aneuploidies. In the experiments described above, each titan cell produced progeny that could grow under fluconazole stress conditions and the resulting populations contained variable suites of aneuploid chromosomes. We next asked whether this variability extended to sibling daughter cells produced by the same titan mother. We utilized sequential microdissection to isolate sibling daughter cells from six titan mother cells (Fig. 6A and B) and measured their viability and growth rate under nutrient-replete (YPD; one set of titan cell-derived offspring) and drug stress (YPD plus fluconazole; five sets of titan cell-derived offspring) conditions. Under nutrient-replete conditions, sibling daughter cells produced similarly sized colonies ($T1_{YPD}$) (average area of colony, 2.0 mm^2; range, 1.17 to 2.97 mm^2) (Fig. 6C and D), suggesting that all titan cell daughter strains were viable and had similar growth potentials when not exposed to stress. In contrast, when sibling daughters were grown on 8 μg/ml fluconazole (a level above the MIC of the KN99α parent strain), some sibling strains did not produce a colony whereas those siblings that did grow had very different colony sizes, from very small to 1.5× the size of the largest colony seen on YPD (for $T2_{Flu}$, 0.96 to 5.05 mm^2; for $T3_{Flu}$, 0.08 to 1.9 mm^2; for $T4_{Flu}$, 0.29 to 2.06 mm^2; for $T5_{Flu}$, 0.16 to 3.38 mm^2; for $T6_{Flu}$, 0.10 to 3.12 mm^2) (Fig. 6C and D). Sibling progeny strains thus differed phenotypically, and this result is suggestive of genotypic differences.

To investigate potential genomic differences between the populations resulting from sibling titan daughter cells, we analyzed karyotypic variation with whole-genome sequencing for populations derived from the five titan cell strains isolated on fluconazole described above (T2 to T6) and an additional 7 titan cell strains (T7 to T13) for a total of 43 daughter strains from 12 different titan cell mother strains. Strikingly, multiple aneuploid karyotypes were generated by sibling daughter cells (Fig. 7; see also Fig. S2 in the supplemental material). At the extreme, all three sibling strains isolated from T6 (Fig. 7) were different: strain T6.1 was disomic for Chr1, strain T6.6 was disomic for Chr4, and strain T6.8 was disomic for both Chr4 and Chr10. Interestingly, ~25% of the titan daughter strains seemed to have a base diploid genome. Three siblings from T2 had a chromosome with reduced copy (i.e., monosomy), which is possible only with a base genome that is diploid (at least). An additional nine strains had at least one chromosome with a copy number close to 1.5× that of the base genome (Fig. 7; see also Fig. S2). It is theoretically possible that the 1.5× chromosomal population frequency is achieved through a 50:50 mixed population of haploid euploids and haploid disomes, but a diploid base genome with chromosomal trisomy is more

parsimonious. In two cases (T2.7 and T3.10; Fig. 7), there were two chromosomes at 1.5×; if there were mixed populations with a haploid base genome, both chromosomes would have to have been lost at equal rates (and in 50% of the population). It may be that certain titan cells are more likely to produce diploid daughters than others—all six siblings from T2 were putative diploids. Thus, titan mother cells have the capacity to generate a diverse repertoire of daughter cells carrying different base ploidy states in addition to different types of aneuploidies.

To determine the effect of ploidy and different aneuploid chromosomes on fitness in fluconazole, we measured the MIC of sibling strains with different ploidy and aneuploid karyotypes. All progeny tested had increased MIC_{50} levels compared to the parental strain (Fig. 8). Progeny from T3 (haploid base ploidy) had consistently higher MIC_{50} levels than progeny from T2 (putative diploid base ploidy, with the exception of T2.6). Interestingly, although Chr1 disomy or trisomy was by far the most frequently isolated aneuploidy (26 of 53 strains analyzed), strains carrying other aneuploidies reached MIC levels similar to those of strains with extra copies of Chr1, demonstrating that comparable levels of fluconazole resistance can be achieved by multiple mechanisms.

Titan cells generate haploid daughter cells under nitrosative and oxidative stress conditions. As all but one of the fluconazole-resistant titan daughter strains were aneuploid, we hypothesized that aneuploidy would also explain the survival benefit of titan cell strains under conditions of oxidative and nitrosative stress. We analyzed progeny from titan cells cultured in the presence of oxidative stress and nitrosative stress (6 and 50 progeny populations, respectively) by flow cytometry and performed whole-genome sequencing on 6 oxidative-stress-resistant and 5 nitrosative-stress-resistant titan daughter populations (Fig. 9). Unexpectedly, no aneuploidy or ploidy variation was evident in the whole-genome sequence data from these titan progeny cells. Point mutation rates under nitrosative and oxidative stress conditions were similar to those seen in the nutrient-replete and fluconazole-resistant progeny (see Table S5 in the supplemental material) (note that many of the predicted changes are on Chr11 and likely reflect segregating variation between KN99α, the progenitor strain, and H99, the strain used for sequence alignment). These data suggest that aneuploidy is not positively selective under conditions of nitrosative and oxidative stresses. Furthermore, since titan progeny populations are better able to grow following exposure to these stresses (Fig. 1), this indicates that there must be additional mechanisms, aside from aneuploidy, that can enhance stress resistance in titan progeny relative to typical cell progeny.

DISCUSSION

Enlarged cryptococcal cells have been observed in human pulmonary infections since the 1970s (7), but recently these polyploid titan cells have begun to be analyzed in detail (4, 9). Titan cells, which are thought to arise via endoreplication (48, 49), play an important role in establishment of the initial pulmonary infection, subsequent dissemination to the central nervous system, and overall virulence (3, 4, 11, 12), and yet little is known about the underlying molecular and genetic mechanisms by which titan cells contribute to disease. Here we isolated single titan cells and titan daughter cells to examine how populations initiated from titan cell strains were able to adapt to a range of stress conditions. Separate analyses of titan and typically sized (typical) cells revealed that the titan cell population had a growth advantage under three different stress conditions (oxidative, nitrosative, and fluconazole).

Populations derived from individual titan cells were six times more likely to form colonies in the presence of fluconazole than typical cryptococcal cells (Table 1). Similar results were observed in liquid culture, where populations initiated from titan cells achieved higher growth than populations from typical cells at high levels of fluconazole (Fig. 1A; ~2% survival advantage relative to typical cells). Importantly, this survival growth advantage was maintained when we isolated the normally sized daughters of titan cells grown in the presence of fluconazole (a 9-fold increase in population size if we correct for the number of cells that grew in YPD; a 12-fold increase without correction). Thus, although the difference between titan and typical cells in the numbers of offspring produced may appear minor (see, e.g., Fig. 1A), the significant advantage seen with the titan cells is more evident at the single-cell level (Table 1). Furthermore, this advantage is passed on and magnified in their offspring when growth in fluconazole is maintained (Fig. 2A). As cryptococcal populations can be quite large *in vivo*, even a small numerical advantage has the potential to increase the efficacy of selection and the likelihood that resistant mutants would arise within the population.

The genomic changes that facilitated the growth of resistant populations in fluconazole were identified by whole-genome sequencing. We macromanipulated 17 titan cells onto fluconazole and then microdissected sequential daughter cell strains from 12 of them. We resequenced the whole genomes of cells isolated from the resultant colonies of the first 5 titan cell populations and of 43 titan cell daughter strains. Whole-chromosomal aneuploidy was detected in 46 of the 48 different strains, while 1 of the original titan cell populations contained an isochromosome of Chr1R. Furthermore, although the majority of strains had a haploid base genome, 12 (25%) putative diploid strains originating from seven different titan mother cells were also isolated. Very few point mutations were acquired in either the presence or the absence of stress, as expected given the low number of cell divisions that had ensued (~20 cell divisions during colony formation [50] and ~8 generations to grow a colony overnight in liquid medium prior to sequencing). The low point mutation rate highlights the high rate at which aneuploidy appeared and the strong selective advantage that enabled aneuploid isolates to sweep through the titan cell daughter populations that were maintained in the presence of fluconazole.

The rapid genome reduction seen with polyploid titan cells occurred within a very small number of cell divisions. The cellular mechanism that mitotically produces genomic variants from polyploid parental cells in *C. neoformans* remains unknown. Studies of *S. cerevisiae*, *C. albicans*, and mammalian cells suggest two possible routes to aneuploidy: (i) chromosome missegregation due to syntelic attachments where the two sister chromosomes attach to the same spindle pole due to distortions of the spindle geometry caused by the polyploidy (51) and (ii) defects in chromosome segregation due to multiple centrosomes/spindle pole bodies per cell (32). In *C. albicans* populations grown in fluconazole, tetraploids form through a mitotic defect and retain two mitotic spindles. The presence of multiple spindles in the tetraploids drives unequal chromosome segregations that produce subpopulations of cells that are aneuploid as well as an appreciable subpopulation whose members are inviable (52). Whether titan daughter cell populations also produce intermediate karyotypes

remains unknown. The observation that all titan daughter cells generated in the absence of stress are viable haploids suggests that missegregation is not typical during titan cell division. Since not all stresses induced aneuploidy as the mechanism of resistance, it is also possible that missegregation, and production of nonviable intermediates, is a specific consequence of fluconazole exposure. We identified several sibling cells that did not grow in fluconazole, but we were unable to differentiate between drug resistance and lack of viability in our system. Importantly, a single polyploid titan mother cell grown in fluconazole produced daughter cell populations with several different aneuploid karyotypes, indicating that the mechanism that produces aneuploid daughters from polyploid titan mothers is not entirely deterministic.

A relationship between aneuploidy and stress response has been observed in previous studies of fungal microbial species under a range of conditions (39, 42, 53). We propose that the key change producing fluconazole resistance in titan daughter cells is ploidy variation and aneuploidy in particular. The most frequent aneuploidies identified in the titan cell progeny were disomy for all or part of Chr1 and/or disomy of Chr4. Extra copies of chromosomes 6, 8, and 10 also appeared in a smaller number of strains, always in the presence of a second extra chromosome or in a putative diploid (rather than haploid) genome. Less frequently, and only in putative diploids derived from the same titan cell, we observed loss of chromosomes 9 and 13. Taken together, these data are consistent with the observation that chromosomes 1, 4, 10, and 11 are frequently found in fluconazole-resistant strains of *C. neoformans* (42) and suggest that the suite of aneuploidies that appears and is selected in titan cell daughters are very similar to those aneuploidies previously identified under fluconazole stress conditions. Unlike previous studies that were initiated with haploids, however, a large number of the titan daughter cells carried multiple aneuploidies. Furthermore, we did not detect a correlation between the number of disomic chromosomes and MIC in the titan progeny. Aneuploidy is unstable in most organisms, including *C. neoformans*. Aneuploid and diploid hybrid strains formed by crossing *C. neoformans* var. *grubii* and *C. neoformans* var. *neoformans* are unstable and frequently undergo loss of individual chromosomes (54). Fluconazole-resistant aneuploid strains frequently return to the haploid state when fluconazole stress is removed (42), and studies performed with human clinical isolates show differences in fluconazole resistance based on the length of exposure to fluconazole within the laboratory (55, 56).

That titan progenies exposed to oxidative and nitrosative stress conditions do not show evidence of aneuploidy is intriguing, as titan cell populations showed a significant survival and growth advantage at multiple levels of these stressors. These data suggest that aneuploidy is not an available beneficial response to these stressors. Furthermore, only a single amino acid change was identified among 11 sequenced titan cell offspring isolated from nitrosative and oxidative stress conditions (in an uncharacterized protein; see Table S5 in the supplemental material). It thus seems likely either that undetected structural genomic changes have arisen in these populations or that titan cells provide their offspring with an epigenetic or physiological advantage under some stress conditions. Of course, in addition to aneuploidy, such mechanisms could also contribute to fluconazole resistance of the titan progeny. It is also important to note that the fluconazole treatment could be causing the observed aneuploidy and that this may not be a normal response to other stresses.

Titan cell production is primarily observed during interactions with eukaryotic host organisms such as humans, mammals, and insects (4, 7, 57). Titan cells are produced within 1 day after the cryptococcal cells enter the host (4). We envision that the response to this new environment triggers titan formation and that titan cells subsequently divide to produce multiple haploid (or diploid) daughter cells, all with potentially different karyotypes. This could provide a high degree of genetic variation relatively rapidly and could do so at a rate significantly higher than that seen with the long time scales required for beneficial mutations to appear and become established within the small clonal founding population. Aneuploidy, such as that seen in clinical isolates (45, 56) and with fluconazole stress, may permit cryptococcal populations to survive and adapt to the range of new environmental challenges found in the host. Importantly, because aneuploidy is much less stable than genomic mutations, it is easily reversible, and thus chromosomes can either be gained or lost very quickly, providing a wide range of diversity upon which selection can act. The transition from polyploid titan cells to haploidy may also increase the chromosomal rearrangement rate, and future work should determine whether such rearrangements are present within the titan daughter populations resistant to oxidative and nitrosative stress.

Understanding how titan cells generate genetically and karyotypically diverse progeny will facilitate the development of new therapeutic strategies aimed at blocking these ploidy transitions. For example, a genome-wide screen in *S. cerevisiae* identified genes essential for the viability of polyploid cells (51). Development of antifungal drugs that target the essential processes necessary for titan cell formation or subsequent division would limit the ability of *C. neoformans* to adapt to the host environment, ultimately limiting disease progression.

Titan cell progeny clearly have a range of potential karyotypes, demonstrating the plasticity of the *C. neoformans* genome and the ability of *C. neoformans* to tolerate chromosomal imbalances and genomic rearrangements under certain conditions. The dramatic titan cell phenotype makes *C. neoformans* an excellent model system for the study of genome plasticity, as cells undergoing genomic changes are readily identifiable and trackable. In addition, these results highlight the need for novel techniques to study single cells in real time and to follow how they rapidly adapt to changing environments—whether that environment is inside a host for pathogens, in response to global warming for environmental organisms, or due to changes in microbiome or metabolism for mammalian cancer cells.

MATERIALS AND METHODS

Ethics statement. Mice were handled in accordance with guidelines defined by the University of Minnesota Animal Care and Use Committee (IACUC), under approved protocol numbers 1010A91133 and 1308-30852. All animal experiments were done in concordance with the Animal Welfare Act, United States federal law, and NIH guidelines.

Production and isolation of titan cells. *C. neoformans* var. *grubii* strain KN99α (58) was grown at 30°C in yeast extract-peptone-dextrose (YPD) agar or broth medium (BD, Hercules, CA) overnight. Cells were collected by centrifugation, washed with phosphate-buffered saline (PBS), and resuspended in sterile saline solution. Groups of 6- to 8-week-old female A/J or C57BL/6J mice (Jackson Laboratory, Bar Harbor, MA) were anesthetized by intraperitoneal pentobarbital injection and infected intranasally with 5×10^6 cells in a 25-μl volume. At 3 to 5 days postinfection, mice were sacrificed by CO_2 inhalation, a needle was placed into the trachea, and lungs were lavaged with 1.5 ml sterile PBS three times.

Cells harvested by bronchoalveolar lavage (BAL) were centrifuged at 12,000 × g for 1 min. To lyse host cells, samples were resuspended in 0.05% SDS–sterile water and subjected to vortex mixing. Cells were then washed twice with sterile water and resuspended in PBS. To separate titan and normally sized (which we refer to as "typical") cell populations, washed BAL fluid samples were filtered using CellMicroSieves (BioDesign Inc. of New York, Carmel, NY) with a 20-μm pore size. The CellMicroSieves were then rinsed with PBS to remove typical cells from the filter. To recover the titan cell population, the CellMicroSieves were inverted and the membrane was washed with PBS. The resulting titan cell population was concentrated by centrifugation at 12,000 × g for 1 min. To recover the typically sized cell population, the filter flowthrough was concentrated by centrifugation at 12,000 × g for 1 min.

To purify single titan or typical cells, washed BAL fluid samples were deposited onto the top quarter of a YPD agar plate. Cells were individually microdissected using an Axioskop tetrad 40 microscope (Carl Zeiss, Jena, Germany) (typical cells) or macrodissected with a Wild M5 stereomicroscope (Wild Heerbrugg AG, Switzerland) (titan cells) to the lower half of the plate, followed by incubation at 30°C for 48 h to generate colonies.

To isolate individual titan daughter cells, macrodissected titan cells were incubated at 30°C for approximately 8 h or until the first cell division. Single titan daughter cells were isolated from the mother titan cell using microdissection. Plates were incubated at 30°C for 48 to 96 h until colonies developed. The size of resultant colonies was measured through the "Analyze particles" macro in ImageJ.

Stress resistance assays. To measure resistance to nitrosative and oxidative stress, titan and typical cell populations (10,000 cells) were inoculated in 100 μl of RPMI medium, at pH 5.0, supplemented with 10% fetal bovine serum (FBS) (ATCC, Manassas, VA), 2% glucose (BD), 1 mM sodium pyruvate (Invitrogen, Carlsbad, CA), 0.01 M HEPES (MP Biomedicals, Solon, OH), 5% penicillin/streptomycin (Invitrogen), and 0.05 mM β-mercaptoethanol (Chemicon), with or without stress (for nitrosative stress, 1.25, 2.5, 5, 10, and 20 mM sodium nitrite [$NaNO_2$] [Sigma-Aldrich]; for oxidative stress, 0.75, 1.5, 3, 6, and 12 mM stabilized hydrogen peroxide [H_2O_2] [Walgreens Co., Deerfield, IL]). At 16 h posttreatment, 10-fold dilutions of each culture were plated onto YPD agar for CFU enumeration. To measure resistance to fluconazole stress, titan and typical cell populations (1,000 cells) were inoculated into YPD medium with 0, 2, 4, 8, 16, 32, 64, 128, 256, or 512 μg/ml fluconazole. After 24 h of incubation at 30°C, each culture was plated onto YPD agar for CFU enumeration. Titan and typical cell populations were also inoculated simultaneously into supplemented RPMI medium or YPD medium (as appropriate). The percentage of survival was calculated as follows: (number of cells under stress conditions/number of cells without stress) ×100. Data were analyzed for each stressor through a two-way ANOVA using cell type (titan or typical) and stress level and their interactions in the model. A full model with all stress levels was tested first. If the results obtained with this model were not significant, sequential models were tested that split the data into low-stress and high-stress groups (see Table S1 in the supplemental material). Data presented are representative of results of three independent experiments from one mouse per experiment.

Single titan and typical cells were purified from BAL fluid samples using microdissection onto YPD agar (control) or YPD agar supplemented with 8 μg/ml fluconazole and incubated at 30°C for 48 to 96 h, and the number of colonies was enumerated. Data are representative of results of three independent experiments from one mouse per experiment.

Determinations of survival and growth of populations initiated from typical cells and normally sized daughters of titan cells in repeated exposure to fluconazole were initiated as described above. Titan and typical cell populations acquired from BAL fluid were split, and 10,000 cells of each were inoculated (separately) into 100 μl of YPD or YPD supplemented with 128 μg/ml fluconazole. After 24 h of incubation at 30°C, cells from each treatment were diluted and plated onto YPD plates. The remaining samples from the YPD-plus-fluconazole treatments were transferred into fresh medium and filtered to remove any titan cells. The filtered normally sized cells derived from titan cells and typical cells were centrifuged to remove the supernatant and added to YPD or YPD plus fluconazole. After 24 h of incubation at 30°C, each sample was again diluted and plated onto YPD plates. YPD plates were always incubated at 30°C for 48 h prior to counting CFUs. The total number of cells plated was determined, and the number of cells that grew after exposure to fluconazole was standardized using the number of CFU determined after growth in YPD (i.e., no drug control). Data presented are representative of results of four independent experiments from one mouse per experiment; statistical assessment was conducted on the full set of data, with experimental day as a factor in the model.

To determine MICs in fluconazole, overnight cultures of KN99α colonies, colonies from macrodissected titan cells, and colonies derived from individual titan daughter cells were washed twice with PBS and diluted to a final concentration of 2.5×10^4 cells/ml in RPMI 1640 medium (with L-glutamine and bicarbonate [pH 7.0]) supplemented with 0, 2, 4, 8, 16, 32, 64, 128, 256, or 512 μg/ml fluconazole. The optical density at 600 nm (OD_{600}) was measured before (OD_{0h}) and after (OD_{72h}) incubation at 30°C in 5% CO_2 for 72 h. Mean OD data were obtained from triplicate samples. Percent survival was calculated as follows: [$\Delta OD_{(72h-0h)}$ (treated)/$\Delta OD_{(72h\text{-}0h)}$ (untreated)] × 100. MIC_{50} and MIC_{90} values were defined as the lowest concentration of drug that resulted in 50% and 90% reductions of growth, respectively. Data are representative of results of three independent biological experiments.

Ploidy determination by flow cytometry. That ploidy of titan cell progeny was different from that of titan cells was initially determined by flow cytometry. Log-phase cultures were harvested by centrifugation at 12,000 × g, fixed in 3.7% formaldehyde at room temperature for 30 min, and washed with PBS. Fixed cells were resuspended in PBS at a concentration of approximately 1×10^6 cells/ml and sonicated for 10 s three times. Cells were stained with 300 ng/ml DAPI (4′,6-diamidino-2-phenylindole) (Invitrogen, Carlsbad, CA) at room temperature for 15 min and then washed with PBS. Flow cytometry was performed on 10,000 cells using an LSR II flow cytometer (Becton, Dickinson, Hercules, CA). The fluorescence of unstained fixed cells was used to establish the baseline, and log-phase KN99α cells grown in YPD were used as a control to identify haploid cell populations (4). Flow cytometric data were analyzed using FlowJo software (Treestar, Ashland, OR).

Analysis of aneuploidy. To examine karyotypes using pulsed-field gel electrophoresis, fluconazole-resistant strains were grown in yeast nitrogen base (YNB) medium supplemented with 1 M NaCl and 8 μg/ml fluconazole at 30°C until an optical density at 600 nm of 0.5 was reached. Strain KN99α grown in YNB medium without fluconazole was used as a haploid control. Cells were harvested and agarose-embedded intact chromosomal DNA was prepared as described previously (59). Samples were run in a 1% agarose gel using 0.5× Tris-borate-EDTA (TBE) running buffer and a CHEF-DR III apparatus (Bio-Rad, Richmond, CA). Gel electrophoresis settings were as follows: 7- to 100-s switch, 4.5 V/cm, and 120° angle (for 21 h), followed by 80- to 400-s switch, 3.5 V/cm, and 120° angle (for 21 h). Chromosomes were stained and visualized with ethidium bromide. Southern blot analysis was performed using a 505-bp probe corresponding to the CNAG_00385.2 gene on the right arm of chromosome 1. The probe was generated using PCR amplification with primers KN0463 (5′ CAT AGG GAA GAC TGA TAG CTG 3′) and KN0464 (5′ GCT GTG GTG CTG GGA ACA AG 3′) and labeled with digoxigenin-11–dUTP (DIG-11-dUTP) (Roche, Lewes, United Kingdom).

Cell karyotypes were also analyzed by quantitative PCR. qPCR primers were designed to amplify 100 bp on one arm of each of the 14 cryptococcal chromosomes. All primers were searched using BLAST to ensure their uniqueness and validated by 10-fold serial dilution to determine that the amplification efficiency was close to 2. Sequences, chromosomal locations, amplicon sizes, and the amplification efficiency of the primers used in this study are provided in Table S2 in the supplemental material. qPCR reactions were performed in an iQ5 real-time PCR detection system (Bio-

Rad) using 15-μl reaction volumes. All reactions were set up in technical triplicate. Each reaction mixture contained 2× iQ SYBR green supermix (Bio-Rad), 300 nM (each) primer, 5-ng genomic DNA from CTAB extraction, and distilled water (dH_2O). Cycling conditions were 95°C for 5 min followed by 40 cycles of 95°C for 15 s and 55°C for 1 min. Melt curve analysis was performed in 0.5°C increments from 55 to 95°C for 5 s for each step to verify that no primer dimers or product from misannealed primers had been amplified. Threshold cycle (C_T) values were obtained using iQ5 optical system software version 2.0 (Bio-Rad) where the threshold was adjusted to be within the geometric (exponential) phase of the amplification curve. Chromosome copy numbers were determined using a modified version of the classical $\Delta\Delta C_T$ method as described by Pavelka et al. (38). Aneuploidy was also determined using multiplex PCR as described by Ni et al. (60). The primers for multiplex PCR are listed in Table S3.

Whole-genome sequencing. Colonies from purified single titan cells and titan daughter cells were randomly selected and inoculated in 50 ml YPD supplemented with 8 μg/ml fluconazole and in RPMI medium supplemented with 3 mM H_2O_2 or 10 mM $NaNO_2$ for overnight culture at 30°C. Genomic DNA was prepared using cetyltrimethylammonium bromide (CTAB) phenol-chloroform extraction as described previously (61). Genomic DNA was further purified using a PowerClean DNA cleanup kit (Mo Bio). Genomic DNA was then fragmented, and library preparation was performed by the DNA sequencing core at the Mayo Clinic (Rochester, MN) using standard Illumina protocols and Illumina paired-end adapters. Paired-end 100-cycle multiplex sequencing was performed on an Illumina Hiseq 2000 sequencer (Illumina, San Diego, CA).

The paired-end fastq files were aligned against the *C. neoformans* var. *grubii* H99 genome (http://www.broadinstitute.org/annotation/genome/cryptococcus_neoformans/) using the Ymap analysis pipeline (14). The read depth for each mapped base pair was determined, and the average number of reads per mapped base pair was calculated for each chromosome. Chromosomal copy numbers were assigned by comparing the average number of reads per chromosome in the subject strain to the average number of reads per chromosome in the resequenced KN99α haploid progenitor strain used for all experiments.

SUPPLEMENTAL MATERIAL

Supplemental material for this article may be found at http://mbio.asm.org/lookup/suppl/doi:10.1128/mBio.01340-15/-/DCSupplemental.

Figure S1, PDF file, 0.1 MB.
Figure S2, PDF file, 0.1 MB.
Table S1, PDF file, 0.03 MB.
Table S2, PDF file, 0.1 MB.
Table S3, PDF file, 0.1 MB.
Table S4, PDF file, 0.1 MB.
Table S5, PDF file, 0.1 MB.

ACKNOWLEDGMENTS

We thank Darren Abby for help with the Ymap analysis, the University of Minnesota Flow Cytometry Core Facility, the Molecular Biology Core at Mayo Clinic, and the University of Minnesota Genomics Center.

This work was supported by National Institutes of Allergy and Infectious Disease R01AI080275 grant to K.N., R01AI0624273 grant to J.B., an ERC Advanced Award 340087/RAPLODAPT to J.B., and NHMRC grant APP1049719 to J.A.F. A.C.G. is grateful to the Azrieli Foundation for the award of an Azrieli Fellowship and was supported by a National Sciences and Engineering Research Council of Canada postdoctoral fellowship and a Banting Fellowship from the Canadian Institutes of Health Research.

REFERENCES

1. **Idnurm A, Bahn Y, Nielsen K, Lin X, Fraser JA, Heitman J.** 2005. Deciphering the model pathogenic fungus Cryptococcus neoformans. Nat Rev Microbiol **3:**753–764. http://dx.doi.org/10.1038/nrmicro1245.
2. **Hu G, Cheng P, Sham A, Perfect JR, Kronstad JW.** 2008. Metabolic adaptation in Cryptococcus neoformans during early murine pulmonary infection. Mol Microbiol **69:**1456–1475. http://dx.doi.org/10.1111/j.1365-2958.2008.06374.x.
3. **Crabtree JN, Okagaki LH, Wiesner DL, Strain AK, Nielsen JN, Nielsen K.** 2012. Titan cell production enhances the virulence of Cryptococcus neoformans. Infect Immun **80:**3776–3785. http://dx.doi.org/10.1128/IAI.00507-12.
4. **Okagaki LH, Strain AK, Nielsen JN, Charlier C, Baltes NJ, Chrétien F, Heitman J, Dromer F, Nielsen K.** 2010. Cryptococcal cell morphology affects host cell interactions and pathogenicity. PLoS Pathog **6:**e1000953. http://dx.doi.org/10.1371/journal.ppat.1000953.
5. **Zaragoza O, Nielsen K.** 2013. Titan cells in Cryptococcus neoformans: cells with a giant impact. Curr Opin Microbiol **16:**409–413. http://dx.doi.org/10.1016/j.mib.2013.03.006.
6. **Love GL, Boyd GD, Greer DL.** 1985. Large Cryptococcus neoformans isolated from brain abscess. J Clin Microbiol **22:**1068–1070.
7. **Cruickshank JG, Cavill R, Jelbert M.** 1973. Cryptococcus neoformans of unusual morphology. Appl Microbiol **25:**309–312.
8. **Wang JM, Zhou Q, Cai HR, Zhuang Y, Zhang YF, Xin XY, Meng FQ, Wang YP.** 2014. Clinicopathological features of pulmonary cryptococcosis with cryptococcal titan cells: a comparative analysis of 27 cases. Int J Clin Exp Pathol **7:**4837–4846.
9. **Zaragoza O, García-Rodas R, Nosanchuk JD, Cuenca-Estrella M, Rodríguez-Tudela JL, Casadevall A.** 2010. Fungal cell gigantism during mammalian infection. PLoS Pathog **6:**e1000945. http://dx.doi.org/10.1371/journal.ppat.1000945.
10. **Wiesner DL, Specht CA, Lee CK, Smith KD, Mukaremera L, Lee ST, Lee CG, Elias JA, Nielsen JN, Boulware DR, Bohjanen PR, Jenkins MK, Levitz SM, Nielsen K.** 2015. Chitin recognition via chitotriosidase promotes pathologic type-2 helper T cell responses to cryptococcal infection. PLoS Pathog **11:**e1004701. http://dx.doi.org/10.1371/journal.ppat.1004701.
11. **Okagaki LH, Nielsen K.** 2012. Titan cells confer protection from phagocytosis in Cryptococcus neoformans infections. Eukaryot Cell **11:**820–826. http://dx.doi.org/10.1128/EC.00121-12.
12. **Okagaki LH, Wang Y, Ballou ER, O'Meara TR, Bahn Y-, Alspaugh JA, Xue C, Nielsen K.** 2011. Cryptococcal titan cell formation is regulated by G-protein signaling in response to multiple stimuli. Eukaryot Cell **10:**1306–1316. http://dx.doi.org/10.1128/EC.05179-11.
13. **Ezov TK, Boger-Nadjar E, Frenkel Z, Katsperovski I, Kemeny S, Nevo E, Korol A, Kashi Y.** 2006. Molecular-genetic biodiversity in a natural population of the yeast Saccharomyces cerevisiae from "Evolution Canyon": microsatellite polymorphism, ploidy and controversial sexual status. Genetics **174:**1455–1468. http://dx.doi.org/10.1534/genetics.106.062745.
14. **Abbey DA, Funt J, Lurie-Weinberger MN, Thompson DA, Regev A, Myers CL, Berman J.** 2014. YMAP: a pipeline for visualization of copy number variation and loss of heterozygosity in eukaryotic pathogens. Genome Med **6:**100. http://dx.doi.org/10.1186/PREACCEPT-1207699561372700.
15. **Anderson CA, Roberts S, Zhang H, Kelly CM, Kendall A, Lee C, Gerstenberger J, Koenig AB, Kabeche R, Gladfelter AS.** 2015. Ploidy variation in multinucleate cells changes under stress. Mol Biol Cell **26:**1129–1140. http://dx.doi.org/10.1091/mbc.E14-09-1375.
16. **Otto SP, Whitton J.** 2000. Polyploid incidence and evolution. Annu Rev Genet **34:**401–437. http://dx.doi.org/10.1146/annurev.genet.34.1.401.
17. **Otto SP, Gerstein AC.** 2008. The evolution of haploidy and diploidy. Curr Biol **18:**R1121–R1124. http://dx.doi.org/10.1016/j.cub.2008.09.039.
18. **Cavalier-Smith T.** 1978. Nuclear volume control by nucleoskeletal DNA, selection for cell volume and cell growth rate, and the solution of the DNA C-value paradox. J Cell Sci **34:**247–278.
19. **Pandit SK, Westendorp B, de Bruin A.** 2013. Physiological significance of polyploidization in mammalian cells. Trends Cell Biol **23:**556–566. http://dx.doi.org/10.1016/j.tcb.2013.06.002.
20. **Lu P, Prost S, Caldwell H, Tugwood JD, Betton GR, Harrison DJ.** 2007. Microarray analysis of gene expression of mouse hepatocytes of different ploidy. Mamm Genome **18:**617–626. http://dx.doi.org/10.1007/s00335-007-9048-y.
21. **Rancati G, Pavelka N, Fleharty B, Noll A, Trimble R, Walton K, Perera A, Staehling-Hampton K, Seidel CW, Li R.** 2008. Aneuploidy underlies rapid adaptive evolution of yeast cells deprived of a conserved cytokinesis motor. Cell **135:**879–893. http://dx.doi.org/10.1016/j.cell.2008.09.039.
22. **Castedo M, Coquelle A, Vivet S, Vitale I, Kauffmann A, Dessen P, Pequignot MO, Casares N, Valent A, Mouhamad S, Schmitt E, Modj-**

tahedi N, Vainchenker W, Zitvogel L, Lazar V, Garrido C, Kroemer G. 2006. Apoptosis regulation in tetraploid cancer cells. EMBO J **25:** 2584–2595. http://dx.doi.org/10.1038/sj.emboj.7601127.
23. **Galitski T, Saldanha AJ, Styles CA, Lander ES, Fink GR.** 1999. Ploidy regulation of gene expression. Science **285:**251–254. http://dx.doi.org/10.1126/science.285.5425.251.
24. **Springer M, Weissman JS, Kirschner MW.** 2010. A general lack of compensation for gene dosage in yeast. Mol Syst Biol **6:**368. http://dx.doi.org/10.1038/msb.2010.19.
25. **Inzé D, De Veylder L.** 2006. Cell cycle regulation in plant development. Annu Rev Genet **40:**77–105. http://dx.doi.org/10.1146/annurev.genet.40.110405.090431.
26. **Storchova Z, Pellman D.** 2004. From polyploidy to aneuploidy, genome instability and cancer. Nat Rev Mol Cell Biol **5:**45–54. http://dx.doi.org/10.1038/nrm1276.
27. **Song K, Lu P, Tang K, Osborn TC.** 1995. Rapid genome change in synthetic polyploids of Brassica and its implications for polyploid evolution. Proc Natl Acad Sci U S A **92:**7719–7723. http://dx.doi.org/10.1073/pnas.92.17.7719.
28. **Mayer VW, Aguilera A.** 1990. High levels of chromosome instability in polyploids of Saccharomyces cerevisiae. Mutat Res **231:**177–186. http://dx.doi.org/10.1016/0027-5107(90)90024-X.
29. **Chen ZJ, Ni Z.** 2006. Mechanisms of genomic rearrangements and gene expression changes in plant polyploids. Bioessays **28:**240–252. http://dx.doi.org/10.1002/bies.20374.
30. **Torres EM, Sokolsky T, Tucker CM, Chan LY, Boselli M, Dunham MJ, Amon A.** 2007. Effects of aneuploidy on cellular physiology and cell division in haploid yeast. Science **317:**916–924. http://dx.doi.org/10.1126/science.1142210.
31. **Lv L, Zhang T, Yi Q, Huang Y, Wang Z, Hou H, Zhang H, Zheng W, Hao Q, Guo Z, Cooke HJ, Shi Q.** 2012. Tetraploid cells from cytokinesis failure induce aneuploidy and spontaneous transformation of mouse ovarian surface epithelial cells. Cell Cycle **11:**2864–2875. http://dx.doi.org/10.4161/cc.21196.
32. **Fujiwara T, Bandi M, Nitta M, Ivanova EV, Bronson RT, Pellman D.** 2005. Cytokinesis failure generating tetraploids promotes tumorigenesis in p53-null cells. Nature **437:**1043–1047. http://dx.doi.org/10.1038/nature04217.
33. **Olaharski AJ, Sotelo R, Solorza-Luna G, Gonsebatt ME, Guzman P, Mohar A, Eastmond DA.** 2006. Tetraploidy and chromosomal instability are early events during cervical carcinogenesis. Carcinogenesis **27:**337–343. http://dx.doi.org/10.1093/carcin/bgi218.
34. **Galipeau PC, Cowan DS, Sanchez CA, Barrett MT, Emond MJ, Levine DS, Rabinovitch PS, Reid BJ.** 1996. 17p (p53) allelic losses, 4N (G2/tetraploid) populations, and progression to aneuploidy in Barrett's esophagus. Proc Natl Acad Sci U S A **93:**7081–7084. http://dx.doi.org/10.1073/pnas.93.14.7081.
35. **Siegel JJ, Amon A.** 2012. New insights into the troubles of aneuploidy. Annu Rev Cell Dev Biol **28:**189–214. http://dx.doi.org/10.1146/annurev-cellbio-101011-155807.
36. **Duesberg P, Stindl R, Hehlmann R.** 2001. Origin of multidrug resistance in cells with and without multidrug resistance genes: chromosome reassortments catalyzed by aneuploidy. Proc Natl Acad Sci U S A **98:**11283–11288. http://dx.doi.org/10.1073/pnas.201398998.
37. **Lee AJX, Endesfelder D, Rowan AJ, Walther A, Birkbak NJ, Futreal PA, Downward J, Szallasi Z, Tomlinson IPM, Howell M, Kschischo M, Swanton C.** 2011. Chromosomal instability confers intrinsic multidrug resistance. Cancer Res **71:**1858–1870. http://dx.doi.org/10.1158/0008-5472.CAN-10-3604.
38. **Pavelka N, Rancati G, Zhu J, Bradford WD, Saraf A, Florens L, Sanderson BW, Hattem GL, Li R.** 2010. Aneuploidy confers quantitative proteome changes and phenotypic variation in budding yeast. Nature **468:**321–325. http://dx.doi.org/10.1038/nature09529.
39. **Selmecki A, Forche A, Berman J.** 2006. Aneuploidy and isochromosome formation in drug-resistant Candida albicans. Science **313:**367–370. http://dx.doi.org/10.1126/science.1128242.
40. **Selmecki A, Gerami-Nejad M, Paulson C, Forche A, Berman J.** 2008. An isochromosome confers drug resistance in vivo by amplification of two genes, ERG11 and TAC1. Mol Microbiol **68:**624–641. http://dx.doi.org/10.1111/j.1365-2958.2008.06176.x.
41. **Pavelka N, Rancati G, Li R.** 2010. Dr Jekyll and Mr Hyde: role of aneuploidy in cellular adaptation and cancer. Curr Opin Cell Biol **22:**809–815. http://dx.doi.org/10.1016/j.ceb.2010.06.003.
42. **Sionov E, Lee H, Chang YC, Kwon-Chung KJ.** 2010. Cryptococcus neoformans overcomes stress of azole drugs by formation of disomy in specific multiple chromosomes. PLoS Pathog **6:**e1000848. http://dx.doi.org/10.1371/journal.ppat.1000848.
43. **Sunshine AB, Payen C, Ong GT, Liachko I, Tan KM, Dunham MJ.** 2015. The fitness consequences of aneuploidy are driven by condition-dependent gene effects. PLoS Biol **13:**e1002155. http://dx.doi.org/10.1371/journal.pbio.1002155.
44. **Ngamskulrungroj P, Chang Y, Hansen B, Bugge C, Fischer E, Kwon-Chung KJ.** 2012. Characterization of the chromosome 4 genes that affect fluconazole-induced disomy formation in Cryptococcus neoformans. PLoS One **7:**e33022. http://dx.doi.org/10.1371/journal.pone.0033022.
45. **Ormerod KL, Morrow CA, Chow EWL, Lee IR, Arras SDM, Schirra HJ, Cox GM, Fries BC, Fraser JA.** 2013. Comparative genomics of serial isolates of Cryptococcus neoformans reveals gene associated with carbon utilization and virulence. G3 (Bethesda) **2013:**113.005660v1. http://dx.doi.org/10.1534/g3.113.005660.
46. **Kelly SL, Lamb DC, Kelly DE, Manning NJ, Loeffler J, Hebart H, Schumacher U, Einsele H.** 1997. Resistance to fluconazole and cross-resistance to amphotericin B in Candida albicans from AIDS patients caused by defective sterol delta5,6-desaturation. FEBS Lett **400:**80–82. http://dx.doi.org/10.1016/S0014-5793(96)01360-9.
47. **Selmecki AM, Dulmage K, Cowen LE, Anderson JB, Berman J.** 2009. Acquisition of aneuploidy provides increased fitness during the evolution of antifungal drug resistance. PLoS Genet **5:**e1000705. http://dx.doi.org/10.1371/journal.pgen.1000705.
48. **Desnos-Ollivier M, Patel S, Spaulding AR, Charlier C, Garcia-Hermoso D, Nielsen K, Dromer F.** 2010. Mixed infections and in vivo evolution in the human fungal pathogen Cryptococcus neoformans. mBio **1:**e00091-10. http://dx.doi.org/10.1128/mBio.00091-10.
49. **Kronstad JW, Attarian R, Cadieux B, Choi J, D'Souza CA, Griffiths EJ, Geddes JMH, Hu G, Jung WH, Kretschmer M, Saikia S, Wang J.** 2011. Expanding fungal pathogenesis: Cryptococcus breaks out of the opportunistic box. Nat Rev Microbiol **9:**193–203. http://dx.doi.org/10.1038/nrmicro2522.
50. **Joseph SB, Hall DW.** 2004. Spontaneous mutations in diploid Saccharomyces cerevisiae: more beneficial than expected. Genetics **168:**1817–1825. http://dx.doi.org/10.1534/genetics.104.033761.
51. **Storchová Z, Breneman A, Cande J, Dunn J, Burbank K, O'Toole E, Pellman D.** 2006. Genome-wide genetic analysis of polyploidy in yeast. Nature **443:**541–547. http://dx.doi.org/10.1038/nature05178.
52. **Harrison BD, Hashemi J, Bibi M, Pulver R, Bavli D, Nahmias Y, Wellington M, Sapiro G, Berman J.** 2014. A tetraploid intermediate precedes aneuploid formation in yeasts exposed to fluconazole. PLoS Biol **12:**e1001815. http://dx.doi.org/10.1371/journal.pbio.1001815.
53. **Chen G, Bradford WD, Seidel CW, Li R.** 2012. Hsp90 stress potentiates rapid cellular adaptation through induction of aneuploidy. Nature **482:**246–250. http://dx.doi.org/10.1038/nature10795.
54. **Lengeler KB, Cox GM, Heitman J.** 2001. Serotype AD strains of Cryptococcus neoformans are diploid or aneuploid and are heterozygous at the mating-type locus. Infect Immun **69:**115–122. http://dx.doi.org/10.1128/IAI.69.1.115-122.2001.
55. **Sionov E, Chang YC, Kwon-Chung KJ.** 2013. Azole heteroresistance in Cryptococcus neoformans: emergence of resistant clones with chromosomal disomy in the mouse brain during fluconazole treatment. Antimicrob Agents Chemother **57:**5127–5130. http://dx.doi.org/10.1128/AAC.00694-13.
56. **Hu G, Wang J, Choi J, Jung W, Liu I, Litvintseva AP, Bicanic T, Aurora R, Mitchell TG, Perfect JR, Kronstad JW.** 2011. Variation in chromosome copy number influences the virulence of Cryptococcus neoformans and occurs in isolates from AIDS patients. BMC Genomics **12:**526. http://dx.doi.org/10.1186/1471-2164-12-526.
57. **García-Rodas R, Casadevall A, Rodríguez-Tudela JL, Cuenca-Estrella M, Zaragoza O.** 2011. Cryptococcus neoformans capsular enlargement and cellular gigantism during Galleria mellonella infection. PLoS One **6:**e24485. http://dx.doi.org/10.1371/journal.pone.0024485.
58. **Nielsen K, Cox GM, Wang P, Toffaletti DL, Perfect JR, Heitman J.** 2003. Sexual cycle of Cryptococcus neoformans var. grubii and virulence of congenic a and alpha isolates. Infect Immun **71:**4831–4841. http://dx.doi.org/10.1128/IAI.71.9.4831-4841.2003.

59. **Lengeler KB, Fox DS, Fraser JA, Allen A, Forrester K, Dietrich FS, Heitman J.** 2002. Mating-type locus of Cryptococcus neoformans: a step in the evolution of sex chromosomes. Eukaryot Cell **1**:704–718. http://dx.doi.org/10.1128/EC.1.5.704-718.2002.
60. **Ni M, Feretzaki M, Li W, Floyd-Averette A, Mieczkowski P, Dietrich FS, Heitman J.** 2013. Unisexual and heterosexual meiotic reproduction generate aneuploidy and phenotypic diversity de novo in the yeast Cryptococcus neoformans. PLoS Biol **11**:e1001653. http://dx.doi.org/10.1371/journal.pbio.1001653.
61. **Velegraki A, Kambouris M, Kostourou A, Chalevelakis G, Legakis NJ.** 1999. Rapid extraction of fungal DNA from clinical samples for PCR amplification. Med Mycol **37**:69–73. http://dx.doi.org/10.1080/02681219980000101.